BIOCHEMISTRY
including biophysical chemistry & molecular biology

Article

pubs.acs.org/biochemistry

Acetylation of Lysine 92 Improves the Chaperone and Anti-apoptotic Activities of Human αB-Crystallin

Rooban B. Nahomi,[†] Rong Huang,[§] Sandip K. Nandi,[∥] Benlian Wang,[‡] Smitha Padmanabha,[†] Puttur Santhoshkumar,[⊥] Slawomir Filipek,[@] Ashis Biswas,*[,∥] and Ram H. Nagaraj*[,†]

[†]Department of Ophthalmology and Visual Sciences and [‡]Center for Proteomics and Bioinformatics, Case Western Reserve University School of Medicine, Cleveland, Ohio 44106, United States

[§]Department of Medicinal Chemistry, School of Pharmacy, Virginia Commonwealth University, Richmond, Virginia 23298, United States

[∥]School of Basic Sciences, Indian Institute of Technology Bhubaneswar, Bhubaneswar 751013, India

[⊥]Department of Ophthalmology, University of Missouri, Columbia, Missouri 65212, United States

[@]Faculty of Chemistry, University of Warsaw, PL02093 Warsaw, Poland

Supporting Information

ABSTRACT: αB-Crystallin is a chaperone and an anti-apoptotic protein that is strongly expressed in many tissues, including the lens, retina, heart, and kidney. In the human lens, several lysine residues in αB-crystallin are acetylated. We have previously shown that such acetylation is predominant at lysine 92 (K92) and lysine 166 (K166). We have investigated the effect of lysine acetylation on the structure and functions of αB-crystallin by the specific introduction of an N^{ϵ}-acetyllysine (AcK) mimic at K92. The introduction of AcK slightly altered the secondary and tertiary structures of the protein. The introduction of AcK also resulted in an increase in the molar mass and hydrodynamic radius of the protein, and the protein became structurally more open and more stable than the native protein. The acetyl protein acquired higher surface hydrophobicity and exhibited 25−55% higher chaperone activity than the native protein. The acetyl protein had more client protein binding per subunit of the protein and higher binding affinity relative to that of the native protein. The acetyl protein was at least 20% more effective in inhibiting chemically induced apoptosis than the native protein. Molecular modeling suggests that acetylation of K92 makes the "α-crystallin domain" more hydrophobic. Together, our results reveal that the acetylation of a single lysine residue in αB-crystallin makes the protein structurally more stable and improves its chaperone and anti-apoptotic activities. Our findings suggest that lysine acetylation of αB-crystallin is an important chemical modification for enhancing αB-crystallin's protective functions in the eye.

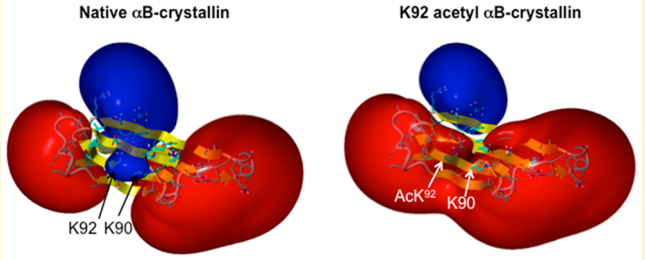

α-Crystallin is a major protein in the human lens and consists of two subunits, αA and αB. These proteins belong to the family of small heat shock proteins that contain a common central core domain of approximately 90 amino acids, known as the "α-crystallin domain" (ACD). The two subunits share significant sequence homology and exist in the lens as hetero-oligomers of varying sizes with an average molecular mass of 800 kDa.[1,2] In the lens, these two proteins function as molecular chaperones.[3] Through direct interaction, these two proteins prevent the aggregation of β- and γ-crystallins, the major proteins of the lens, during aging.[4] α-Crystallin binds to the cytoskeletal proteins actin and vimentin and to filament assembly intermediates,[5−7] and it prevents filament disassembly during cell stress. α-Crystallin also binds to the plasma membrane in lens fiber cells, although the significance of this binding is not known.[8] In addition, α-crystallin binds to microtubules and facilitates microtubule assembly in the lens,[9] and αB-crystallin associates with the centrosome[10] and may participate in cytokinesis during mitosis.[11] Deletion of αA-crystallin or αA- and αB-crystallin together causes cataracts, which are accompanied by the aggregation of proteins.[12,13] Forced expression of chaperone-compromised α-crystallin also leads to cataracts,[14,15] further underlying the importance of α-crystallin's chaperone activity for lens transparency. Outside of the lens, α-crystallin has been shown to bind to β-amyloid and synuclein and prevent their aggregation, which have implications for neurological diseases.[16,17] In addition, the loss of the chaperone activity of αB-crystallin leads to desmin-related cardiomyopathy.[18] Furthermore, αB-crystallin binds to pro-inflammatory cytokines;[19] an immune response against αB-crystallin enhances inflammation in multiple sclerosis,[20] and administration of αB-crystallin reduces the extent of paralysis in

Received: May 21, 2013
Revised: September 9, 2013
Published: October 15, 2013

dx.doi.org/10.1021/bi400638s | *Biochemistry* 2013, 52, 8126−8138

experimental autoimmune encephalomyelitis,[21] which is dependent on its chaperone function.

In addition to its role as a chaperone, α-crystallin is an anti-apoptotic protein[22] that prevents the activation of procaspase-3, binds to Bax, activates PI3-kinase, and inhibits the phosphatase and tensin homologue (PTEN) by directly interacting with those proteins[23,24] and promoting cell survival. There is evidence of such interactions in cells exposed to external stresses.[22]

In the retina, αB-crystallin is present in retinal pigmented epithelial (RPE) cells, Muller cells, retinal capillary cells, and photoreceptors.[22] RPE cells secrete αB-crystallin through an exosomal pathway.[25,26] Although the exact function of the secreted αB-crystallin is not known, αB-crystallin is known to protect RPE cells from oxidative damage.[27] αB-Crystallin could play a role in diabetic retinopathy. Its neuroprotective function becomes weaker in diabetic retinas,[28] which could partly explain early apoptosis in the neural retina during diabetes. α-Crystallin translocates from the cytoplasm to the nucleus when cells are stressed.[29] Whether this nuclear localization is a requirement for its anti-apoptotic function is not known. αB-Crystallin is also present in mitochondria, where it inhibits cytochrome *c* oxidation.[30] Taken together, it is evident that αB-crystallin is a multifaceted protein and plays an important role in preventing superfluous protein denaturation and apoptosis in stressed cells.

Lysine acetylation is a widespread protein modification that occurs in cells. The reaction is catalyzed by lysine acetyl transferases (KATs) in the cytoplasm [and by histone acetyl transferases (HATs) for histones in the nucleus], and deacetylation is regulated by lysine deacetylases (KDACs) [or histone deacetylases (HDACs)].[31,32] While histone acetylation and deacetylation regulate gene expression, lysine acetylation of cytosolic proteins regulates cellular functions and metabolism.[33,34] In the human lens, acetylation of both αA- and αB-crystallin was first reported by Smith's laboratory.[35,36] We have recently identified K70 and K99 in αA-crystallin and K92 and K166 in αB-crystallin as being acetylated in the human lens.[37] We now extend this study to show that αB-crystallin is acetylated in the mouse and human retina (Figure S1 of the Supporting Information). We found that lysine acetylation in α-crystallin improves its chaperone function[37] and that prior lysine acetylation inhibits protein modification by glycation.[38]

Among many lysine residues in human small heat shock proteins (Hsp20, αA- and αB-crystallin, and Hsp27), K92 is highly conserved (Figure S2 of the Supporting Information). Our aim in this study was to determine the specific effects of acetylation at this site on αB-crystallin. To study the effects of acetylation at specific lysine residues on the function of proteins, lysine residues have been mutated to glutamine to mimic acetylation.[39,40] While this mutation replicates the neutralization of the positive charge on the protonated lysine residue, it is not fully structurally compatible with AcK. To circumvent this problem, Huang et al. first described the use of methylthiocarbonyl-aziridine (MTCA) to introduce site-specifically an acetylation mimic into proteins.[41] MTCA reacts with cysteine residues (replacing lysine residues by mutation) in proteins and generates an acetylation mimic, methylthiocarbonyl thialysine (MTCTK). Proteins carrying MTCTK modifications are recognized by the AcK antibody. Furthermore, Huang et al. validated their approach by demonstrating that the introduction of the MTCTK group at K102 of the CK2 protein kinase stimulates its catalytic activity, similar to enzymatic acetylation at these lysine residues.[41] Using the same approach, we have studied the site-specific effect of lysine acetylation at K92 in αB-crystallin. First, we converted K92 to cysteine 92 (C92) by site-directed mutagenesis and introduced an acetylation mimic using MTCA. We report below the impact of acetylation on the structure and function of αB-crystallin.

MATERIALS AND METHODS

Citrate synthase (CS), lysozyme (Lyso), malate dehydrogenase (MDH), protease inhibitor cocktail, methyl chlorothioformate, staurosporine, and etoposide were obtained from Sigma-Aldrich Chemical Co. LLC (St. Louis, MO). Aziridine was purchased from ChemService, Inc. (West Chester, PA). All other chemicals were of analytical grade. γ-Crystallin (GC) from bovine lenses was purified as previously described.[42]

Cloning and Purification of Wild-Type (WT) and Mutant αB-Crystallin. The αB-crystallin (K92C) mutant was amplified using the following primers for cloning: 5′-GGAACTCAAAGTTTGCGTGTTGGGAGATGTG-3′ (forward) and 5′-CACATCTCCCAACACGCAAACTTTGAGTTCC-3′ (reverse). The amplified polymerase chain reaction product was cloned, expressed in *Escherichia coli*, and purified as previously described.[37] The WT protein was similarly purified.[38]

Introduction of the AcK Mimic at the K92 Position of αB-Crystallin. MTCA was synthesized, and the acetylation mimic was introduced at K92 using previously described procedures.[41] Briefly, we added 500 and 200 μL of MTCA (1.0 M solution in acetonitrile) to 5.0 mL of the K92C mutant of αB-crystallin (5.0 mg/mL) and to 2.0 mL of WT αB-crystallin (4.0 mg/mL) in 100 mM ammonium bicarbonate. The mixtures were incubated for 3 h at room temperature. The samples were then dialyzed against 50 mM phosphate buffer (pH 7.5) for 24 h.

Western Blotting for K92 Acetylation in αB-Crystallin. The proteins were separated on a 12% denaturing gel, transferred to a nitrocellulose membrane, and probed with a monoclonal antibody to AcK (Cell Signaling Technologies, Danvers, MA) (1:50000 dilution) and an HRP-conjugated goat anti-mouse IgG (Promega, Madison, WI) (1:5000 dilution). Immunoreactivity was detected using the enhanced chemiluminescence detection kit (Thermo Scientific).

Protein Thiol Assay. The protein thiol assay was performed using the thiol quantification assay kit from Abcam (Cambridge, MA) and a 100 μg protein sample.

Mass Spectrometric Confirmation of K92 Acetylation in αB-Crystallin. The MTCA-derivatized K92C αB-crystallin was subjected to sodium dodecyl sulfate−polyacrylamide gel electrophoresis (SDS−PAGE) on a 12% reducing gel. Gel pieces containing the protein were destained with 50% acetonitrile in 100 mM ammonium bicarbonate followed by 100% acetonitrile for mass spectrometric detection of the AcK mimic, MTCTK. Similarly, MTCA-treated WT αB-crystallin was subjected to electrophoresis and processed. The samples were then treated with 20 mM DTT at room temperature for 60 min followed by treatment with 50 mM iodoacetamide for 30 min in the dark. The reagents were removed, and the gel pieces were washed with 100 mM ammonium bicarbonate and dehydrated in acetonitrile. The gel pieces were then dried in a Speed Vac concentrator (Savant Speed Vac, Thermo Scientific, Rockford, IL), rehydrated in 50 mM ammonium bicarbonate containing sequencing grade modified trypsin, and left to be digested overnight. Proteolytic peptides extracted from the gels with 50% acetonitrile in 5% formic acid were completely dried

in a Speed Vac concentrator and then resuspended in 10 μL of 0.1% formic acid. Three microliters of the peptides was injected into an Orbitrap Elite Hybrid Mass Spectrometer (Thermo Electron, San Jose, CA) equipped with a Waters nanoAcquity ultra-performance liquid chromatography system (Waters, Milford, MA). Liquid chromatography was performed using mobile phase A (0.1% formic acid in water) and mobile phase B (0.1% formic acid in acetonitrile) with a linear gradient of B at an increment of 1%/min at a flow rate of 300 nL/min for 90 min. All spectra were recorded in a positive ion mode using data-dependent methods consisting of a full MS scan (m/z 300−1800) in a high-resolution Orbitrap (resolution of 120000) followed by MS/MS scans of the 15 most abundant precursor ions determined from the full MS scan. The MS/MS spectra were generated in an ion trap with relatively low resolution by collision-induced dissociation of the peptide ions at a normalized collision energy of 35% to generate a series of b and y ions as major fragments. Raw LC−MS/MS data were subjected to a database search using the Mascot search engine (version 2.2.0, Matrix Science) against a protein database containing αB-crystallin sequences and K92C mutated sequences. Oxidized methionine and MTCTK were included as variable modifications. The mass tolerance was set to 10 ppm for the precursor ions and 0.8 Da for the product ions. The significance threshold was $p < 0.05$.

Circular Dichroism Spectroscopy. The far-UV CD spectra were recorded at 25 °C using a Chirascan Plus instrument (Applied Photophysics). The spectra were collected from 190 to 260 nm using a rectangular quartz cell with a 1 mm path length. The proteins (0.2 mg/mL) were dissolved in 50 mM phosphate buffer (pH 7.5). The spectra were analyzed for secondary structure content using CDNN CD spectra deconvolution software (Applied Photophysics). The near-UV CD spectra were measured at 25 °C using the same spectropolarimeter. The spectra were measured with a 1.0 mg/mL protein solution in 50 mM phosphate buffer (pH 7.5). The reported spectra are the average of five scans.

Surface Hydrophobicity and Tryptophan Fluorescence. The surface hydrophobicity of the protein (0.05 mg/mL) was measured using 10 μM 2-*p*-toluidinonaphthalene-6-sulfonate (TNS) (emission at 350−520 nm and excitation at 320 nm). The intrinsic tryptophan fluorescence spectra of the proteins (0.05 mg/mL) in 50 mM phosphate buffer (pH 7.5) at 25 °C were recorded using a Fluoromax 4P spectrofluorometer (Horiba Scientific, Edison, NJ). The excitation wavelength was set to 295 nm, and the emission spectra were recorded between 310 and 400 nm. The data were collected at a 0.5 nm wavelength resolution.

Determination of Structural Stability. The structural stabilities of native αB-crystallin and acetyl αB-crystallin were determined using an equilibrium chemical denaturation experiment. Protein [0.05 mg/mL in 50 mM phosphate buffer (pH 7.5)] was incubated with 0−7 M urea for 18 h at 25 °C. The intrinsic tryptophan fluorescence spectrum of the protein solution was recorded in the 310−400 nm region at an excitation wavelength of 295 nm. The equilibrium unfolding profile was fit according to a three-state model, as described previously.[43]

DLS−MALS Analysis. The samples were injected into a TSK-5000PW$_{XL}$ (Tosoh Bioscience) gel filtration column equilibrated with 50 mM phosphate buffer with 150 mM NaCl buffer (pH 7.2) and connected to an high-performance liquid chromatography system (Shimadzu, Columbia, MD) coupled to multiangle light-scattering and dynamic light-scattering detectors (Wyatt Technology, Santa Barbara, CA). The flow rate was set to 0.75 mL/min. The average molar mass and hydrodynamic radius of the oligomers were determined using ASTRA (Wyatt Technology).

Chaperone Activity Assays. Chaperone activity assays were conducted as previously described.[37] We compared the chaperone activity of WT and MTCA-treated αB-crystallin. The ratios of αB-crystallin to client proteins (w/w) are given in the figure legends. The chaperone activity of αB-crystallin was also assessed in cells transferred with αB-crystallin as previously described.[44] HeLa cells (70% confluent) were transferred with αB-crystallin (4 μg) with the aid of a cationic lipid, BioPORTER (Polyplus transfection reagent, Illkirch, France). A batch of cells treated with BioPORTER alone served as a control. After incubation for 4 h, the cell lysate was prepared using M-PER containing a protease inhibitor cocktail (1:100). Western blotting for αB-crystallin was used to confirm that an equal amount of protein was transferred into the cells. Protein corresponding to 50 μg from cell lysates was either incubated at 55 °C for 2 h or kept at room temperature for 2 h (control). After being incubated, the samples were centrifuged at 14000*g* for 10 min. The protein concentration in the supernatant was measured using the BCA protein assay kit.

Determination of Protein Refolding Ability. MDH (1.0 μM) was denatured in 6 M guanidine hydrochloride (Gu-HCl) for 8 h at 25 °C. Refolding of MDH was initiated by a 100-fold dilution with a refolding buffer [50 mM phosphate buffer, 10 mM magnesium acetate, and 5 mM DTT (pH 7.5)] in the presence or absence of 20 μM native and acetyl αB-crystallin. The MDH concentration was 10 nM during refolding. The activity of the refolded MDH was measured by adding 20 μL of the refolding mixture to 580 μL of refolding buffer containing 0.1 mM NADH and 0.4 mM oxaloacetic acid (preincubated at 25 °C) and measuring the absorbance at 340 nm.

Equilibrium Binding Study. The chaperone−substrate binding study was performed using the membrane filtration method.[45] Briefly, acetyl and native αB-crystallin (12.5 μM) were incubated at 60 °C for 1 h with 2−18 μM GC in 50 mM phosphate buffer (pH 7.5). After equilibration at 25 °C for 1 h, the incubation mixture was spun through a Microcon centrifugal filter device (Millipore, Billerica, MA) (4000*g*) fit with a 100 kDa cutoff membrane filter to separate the unbound substrate. The number of binding sites (n) and the dissociation constant (K_d) were determined as previously described.[45,46]

Apoptosis Measurements. αB-Crystallin was transferred into HeLa cells with the aid of BioPORTER according to the manufacturer's instructions. The cells were cultured in Dulbecco's modified Eagle's medium supplemented with 10% FBS. When the cells were 70−80% confluent, the adherent cells were treated with BioPORTER containing proteins in serum-free medium. Cells treated with BioPORTER alone served as a control. The cells were incubated for 4 h at 37 °C in a humidified 5% CO_2 atmosphere and then washed with PBS. To induce apoptosis, the cells were treated with either 100 nM staurosporine or 20 μM etoposide at 37 °C for 24 h. Early apoptotic cells were detected by staining cells with annexin V-FITC (BD Biosciences, San Jose, CA).

Measurement of Caspase-3 Activity. HeLa cells treated as described above were lysed using M-PER reagent. An equal volume of fluorogenic substrate solution [2× reaction buffer (10 mM DTT and 50 μM Ac-DEVD-AFC)] was added to the cell lysate, which was incubated for 1 h at 37 °C in the dark.

The samples were read in a Spectramax Gemini XPS spectrofluorometer (Molecular Devices, Sunnyvale, CA) at excitation and emission wavelengths of 400 and 505 nm, respectively.

Molecular Modeling. The crystal structure of the ACD (which contains K92) was taken from the Protein Data Bank (entry 2WJ7).[47] The file contains the coordinates of residues 67−157, which are numbered starting at number 4. The structure was renumbered for analysis. Acetylated K92 was built and optimized in YASARA (YASARA Biosciences Inc., Vienna, Austria) employing an Amber03 force field. To visualize the effect of K92 acetylation, the electrostatic potential isosurfaces were calculated at the 25 kcal/mol level. The electrostatic potential was also mapped on the molecular surfaces of WT and K92-acetylated αB-crystallin. All of the calculations and the generation of images were performed in YASARA.

Statistics. The results are presented as means ± the standard deviation (SD). Significant differences among the groups were determined using analysis of variance, and a $p < 0.05$ level was considered significant.

RESULTS

MTCA-mediated introduction of the AcK mimic, MTCTK, occurs specifically on cysteine residues in proteins.[41] The absence of cysteine residues in human αB-crystallin worked to our advantage. We introduced a cysteine residue at K92 and treated the resulting K92C protein with MTCA (Figure 1).

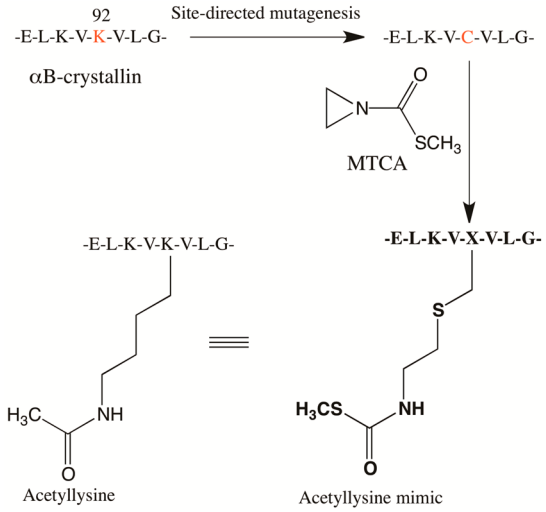

Figure 1. Schematic illustration of the site-specific introduction of an AcK mimic into αB-crystallin. αB-Crystallin mutant K92C was treated with MTCA to generate an AcK mimic at K92. The absence of cysteine residues in αB-crystallin allowed us to introduce an AcK mimic at K92 by first mutating K92 to Cys.

SDS−PAGE of the MTCA-treated WT and K92C protein showed single protein bands similar to unmodified WT and K92C αB-crystallin (Figure 2A). Western blotting using an AcK monoclonal antibody showed reaction with MTCA-modified K92C protein (Figure 2B) but not with untreated WT or K92C protein. MTCA-treated WT protein did not show a reaction. Our procedure resulted in nearly 98% conversion of the cysteine to MTCTK, as revealed using a protein thiol assay (Figure 2C). Mass spectrometric analysis of the peptides derived from the gel band covered approximately 97% of αB-crystallin's sequence. For C92-containing peptides, both unmodified (C92) and modified (AcK mimic at C92) peptide were identified in several trypsin miscut peptides, such as peptides HFSPEELKVCVLGDVIEVHGK (residues 83−103), HFSPEELKVCVLGDVIEVHGKHEER (residues 83−107), and VCVLGDVIEVHGK (residues 91−103). As an example, the tandem mass spectrum of the ion at m/z 495.5900(3+) of the VCVLGDVIEVHGK (residues 91−103) peptide with the AcK mimic is shown in Figure 2D. Compared with that of the unmodified peptide, there is no change in mass for the y series ions from y2 to y11. However, a mass shift of 117 Da was observed for y12, b series ions from b2 to b9, and the precursor ion, which indicates the modification of the C92 residue to MTCTK. Together, these data confirm the specific introduction of the AcK mimic at K92 in αB-crystallin.

Next, we determined whether MTCA treatment alone changes the structure and function of αB-crystallin. WT protein was treated with MTCA (conditions similar to those used for the K92C protein). This treatment changed neither the tryptophan fluorescence (Figure S3A of the Supporting Information) nor the surface hydrophobicity (Figure S3B of the Supporting Information) of the protein and did not alter the secondary structure of αB-crystallin (data not shown). Next, we determined whether MTCA treatment affected the chaperone activity of αB-crystallin. The chaperone activity was assessed using four client proteins, CS, Lyso, MDH, and GC. The client proteins were subjected to thermal (CS, MDH, and GC) or chemical (Lyso) stress to induce protein denaturation. The light scattering from the denatured proteins was monitored spectrophotometrically in the presence or absence of MTCA-treated or untreated αB-crystallin. Both proteins were equally effective against all four client proteins (Figure S3C of the Supporting Information). These results suggest that MTCA treatment alone does not affect the structure or the chaperone activity of αB-crystallin. Because MTCA treatment had no effect on the structure and chaperone activity and because MTCA-mediated conversion of K92C to MTCTK was close to 100%, in all of the subsequent experiments, we used only MTCA-treated K92C and MTCA-treated WT protein for comparison, hereafter termed acetyl and native proteins, respectively.

The far-UV CD spectra for the acetyl and native proteins were nearly identical (Figure 3A). The secondary structural elements of the two proteins are listed in Table 1. The acetyl protein showed marginally higher α-helicity with a slight decrease in the level of β-sheet structure relative to that of the native protein. Near-UV CD spectra of these two proteins revealed that the microenvironments of the aromatic amino acid residues were altered (Figure 3B). The tryptophan fluorescence of the acetyl protein was 33% higher than that of the native protein (Figure 3C), further implying that acetylation perturbed the microenvironment of the tryptophan residues. Taken together, these data show that K92 acetylation had a marginal effect on the secondary structure but had a stronger effect on the tertiary structure of the protein.

In its native state, αB-crystallin exists as a polydisperse oligomer that ranges from 4 to 40 subunits. Whether K92 acetylation affected the oligomeric structure (i.e., quaternary structure) of the protein was investigated using DLS−MALS. As shown in Figure 4A, the acetyl protein had a broader peak than the native protein, with an average molar mass of 9.24×10^5 g/mol compared with a mass of 5.73×10^5 g/mol for the native protein. The hydrodynamic radii (R_h) of the native and acetyl proteins were 8.2 and 10 nm, respectively. Together,

dx.doi.org/10.1021/bi400638s | Biochemistry 2013, 52, 8126−8138

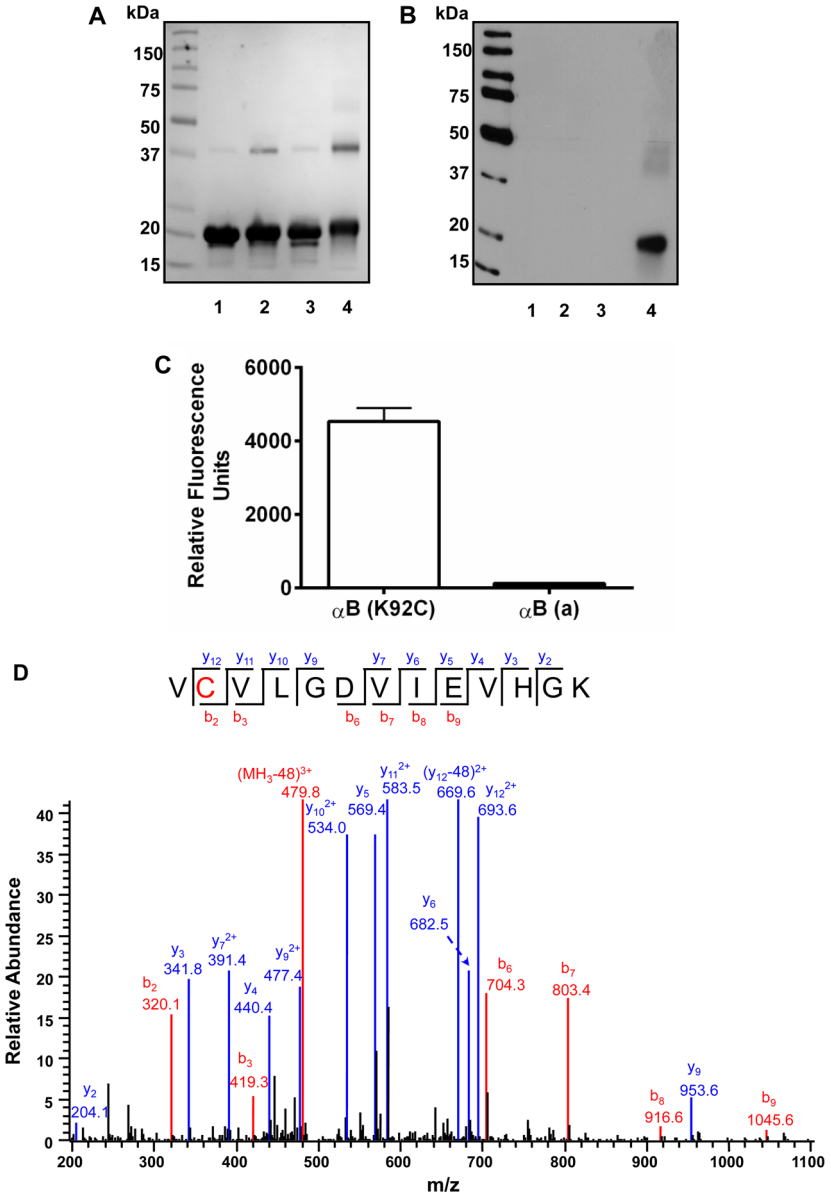

Figure 2. Confirmation of the introduction of the AcK mimic into αB-crystallin. (A) SDS−PAGE of WT (lane 1), K92C (lane 2), WT treated with MTCA (lane 3), and K92C treated with MTCA (lane 4). (B) Western blotting using an AcK antibody showed reaction with only K92C treated with MTCA (lane assignments are the same as in panel A). (C) Estimation of the protein thiol content showed that nearly 98% of the cysteine in the K92C was modified to MTCTK. αB(a) denotes acetyl αB-crystallin. (D) Mass spectrometric identification of the AcK mimic at K92 in αB-crystallin. The tandem mass spectrum of the αB-crystallin peptide [VCVLGDVIEVHGK (residues 91−103)] with a precursor ion at m/z 495.5900(3+) and K92C-modified MTCTK is shown.

these data suggest that K92 acetylation led to an increase in the average oligomeric size, consisting of ∼28 subunits in the native protein to ∼46 subunits in the acetyl protein.

To determine whether an increase in the oligomeric size and the subtle changes in the tertiary structure had any effect on the overall structural stability of the acetyl protein, the thermodynamic stabilities of the native and acetyl proteins were compared. Equilibrium urea unfolding was measured by following the tryptophan fluorescence of these two proteins at various urea concentrations. The λ_{max} values for the native and unfolded WT αB-crystallin were recorded at 340 and 354 nm, and for the acetyl protein at 340 and 352 nm. We plotted the ratio of the intensities in the native and unfolded states as a function of the urea concentration (Figure 4B). An estimate of the transition midpoint ($C_{1/2}$) from the sigmoidal analysis of the denaturation profiles indicated that the $C_{1/2}$ value increased slightly from 2.41 M urea for the native protein to 2.51 M urea for the acetyl protein (Figure 4B and Table 2). To measure the stability against chemical denaturation, all of the profiles were analyzed with the aid of a global three-state fitting procedure according to the following equation:

$$F = [F_N + F_I \exp(-\Delta G_1^\circ + m_1[\text{urea}])/RT + F_U \exp(-\Delta G_2^\circ + m_2[\text{urea}])/RT]/[1 + \exp(-\Delta G_1^\circ + m_1[\text{urea}])/RT + \exp(-\Delta G_2^\circ + m_2[\text{urea}])/RT]$$

where F_N, F_I, and F_U are the fluorescence intensities for the 100% native, 100% intermediate, and 100% unfolded forms,

dx.doi.org/10.1021/bi400638s | Biochemistry 2013, 52, 8126−8138

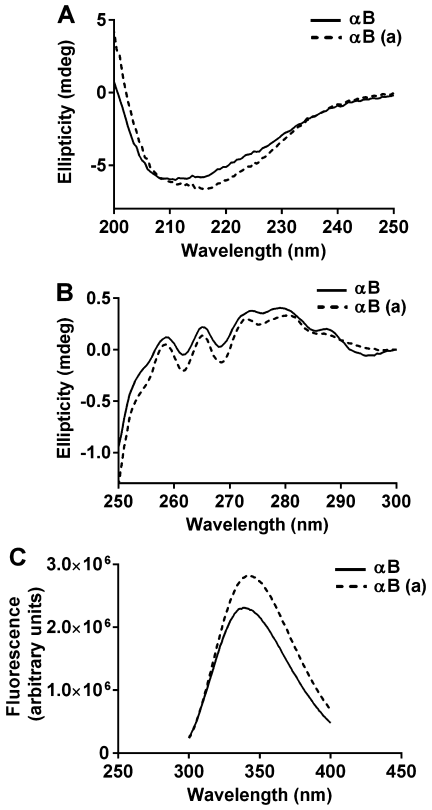

Figure 3. Structural changes in acetyl αB-crystallin. The far-UV (A) and near-UV (B) CD spectra for the native (αB) and acetyl αB-crystallin [αB(a)]. (C) Tryptophan fluorescence was higher for the acetyl protein than for the native protein.

Table 1. Secondary Structural Elements in Native and Acetyl αB-Crystallin

protein	α-helix (%)	β-sheet (%)	β-turn (%)	random coil (%)
native	14.4	38.3	15.8	31.5
acetyl	16.3	34.4	16.1	33.2

respectively. The term ΔG_1° refers to the standard free energy change between the native and intermediate forms, and ΔG_2° refers to the standard free energy change between the intermediate and unfolded forms. The term ΔG° is the sum of ΔG_1° and ΔG_2° and refers to the standard free energy change of unfolding (between the native and unfolded forms) at a urea concentration of zero. The fitted parameters are listed in Table 2. The standard free energy change of the unfolding of the native protein at 25 °C was 22.94 kJ/mol. The ΔG° value for the acetyl protein increased to 29.95 kJ/mol, indicating an increase in thermodynamic stability of approximately 7 kJ/mol.

We then measured the chaperone activity of the protein using the same four client proteins used in the assessment of the effect of MTCA on WT protein (Figure S3C of the Supporting Information). The chaperone activity against CS, Lyso, MDH, and GC was 38, 25, 75, and 66% more effective, respectively, with the acetyl protein than with the native protein (Figure 5A). When tested against CS, the chaperone activity of the acetyl protein was consistently higher than that of the WT protein across various αB-crystallin to client protein ratios (Figure S4 of the Supporting Information). Because only a fraction of the K92 residue in αB-crystallin is acetylated in the human lens,[36] we determined whether a mixture of acetyl and

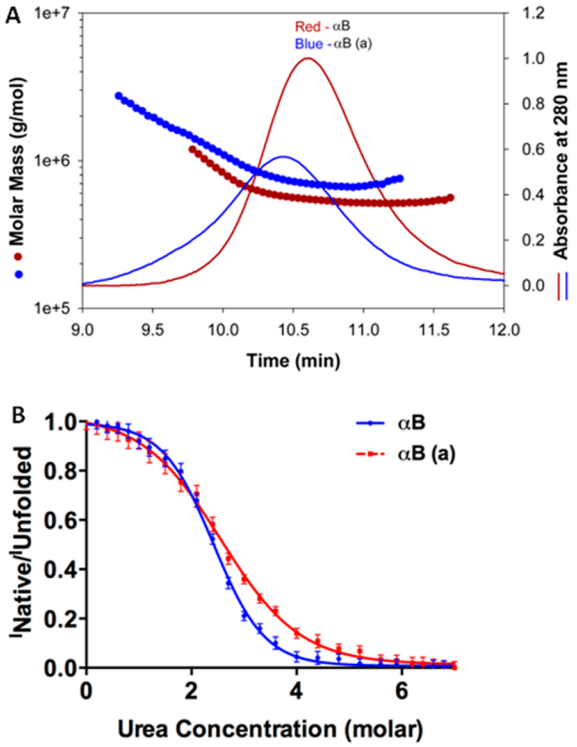

Figure 4. Oligomerization and thermodynamic stability of acetyl αB-crystallin. (A) DLS–MALS profiles for native and acetyl αB-crystallin. The acetyl protein exhibited a larger oligomeric size than the native protein. (B) Equilibrium urea denaturation profile for 0.05 mg/mL native and acetyl αB-crystallin at 25 °C. The profile is normalized to a scale of 0–1. Symbols represent the experimental data points, and the lines represent the best fit according to the three-state model.

Table 2. $C_{1/2}$ and ΔG° Values for Native and Acetyl αB-Crystallin at 25 °C

protein	$C_{1/2}$ (M)	ΔG° (kJ/mol)
native	2.41 ± 0.02	22.94 ± 0.92
acetyl	2.51 ± 0.03	29.95 ± 1.06

native proteins, wherein acetyl protein constituted 1 and 5% of the total protein (1% acetyl + 99% native and 5% acetyl + 95% native), would show an improvement in the chaperone activity (over that of native protein). Remarkably, both mixtures showed significantly higher activity than the native protein against CS. When the sample was tested against GC, only the 5% acetyl + 95% native protein mixture showed a significantly higher activity (Figure 5B,C). Together, these data show that acetylation of K92 improves the chaperone activity of αB-crystallin, and such an improvement in the chaperone activity is maintained even when the acetyl protein makes up a small portion of the total protein.

Next, we compared the ability of the native and acetyl protein to inhibit protein aggregation in HeLa cells. αB-Crystallin was transferred into cells with the aid of BioPORTER. This technique resulted in an equal amount of acetyl and native protein being transferred into the cells, as revealed by Western blotting (Figure 6A). The proteins in the cell lysate aggregated and precipitated as insoluble pellets upon being incubated at 55 °C. We then measured the concentration of the recovered soluble protein in the supernatant. We found a significant difference between the acetyl and native protein in preventing protein aggregation when we used 4 μg of αB-

dx.doi.org/10.1021/bi400638s | Biochemistry 2013, 52, 8126–8138

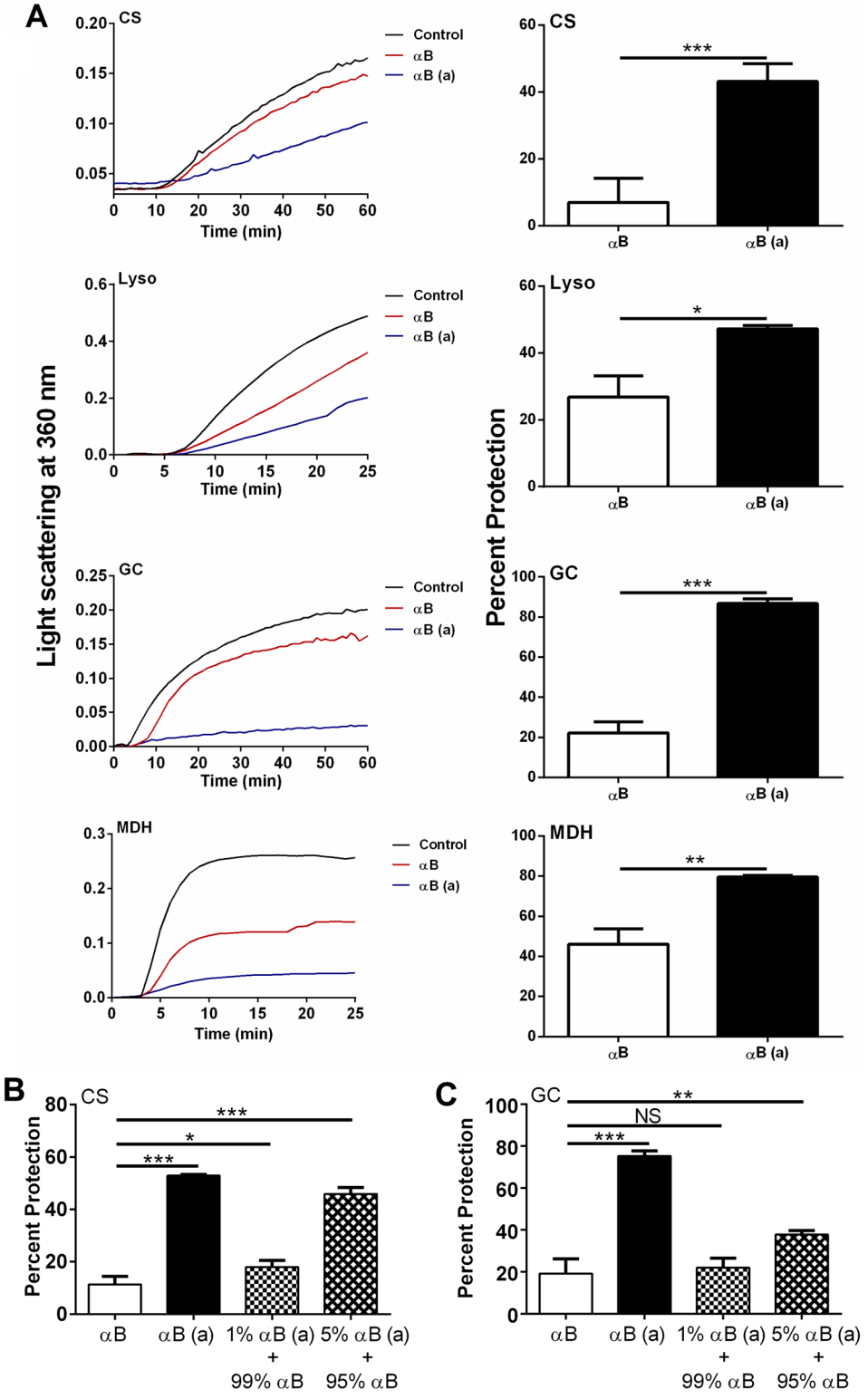

Figure 5. Acetylation of K92 improves the chaperone activity of αB-crystallin. (A) The chaperone activities of the native and acetyl αB-crystallins were measured using citrate synthase (CS), lysozyme (Lyso), γ-crystallin (GC), and malate dehydrogenase (MDH). The following chaperone:client protein ratios (w/w) were used: CS, 1:2; Lyso, 1:4; MDH, 1:8; and GC, 1:6. Representative traces for each assay are shown in the left panels. A mixture of 1% acetyl and 99% native (0.125 μg of acetyl and 12.375 μg of native, 25 μg of CS, 1:2 αB-crystallin:CS ratio) and 5% acetyl and 95% native αB-crystallin (0.625 μg of acetyl and 11.875 μg of native, 25 μg of CS, 1:2 αB-crystallin:CS ratio) significantly improved the chaperone activity against CS (B) and GC (C). αB = native αB-crystallin. αB(a) = acetyl αB-crystallin. Bars are means ± SD of three independent experiments. *p < 0.05. **p < 0.005. ***p < 0.0005. NS means not significant.

crystallin and an incubation time of 2 h (Figure S5 of the Supporting Information). In the controls (without αB-crystallin), there was a 64% loss of protein in the supernatant; however, this value was reduced to 53% with the transfer of the

dx.doi.org/10.1021/bi400638s | Biochemistry 2013, 52, 8126−8138

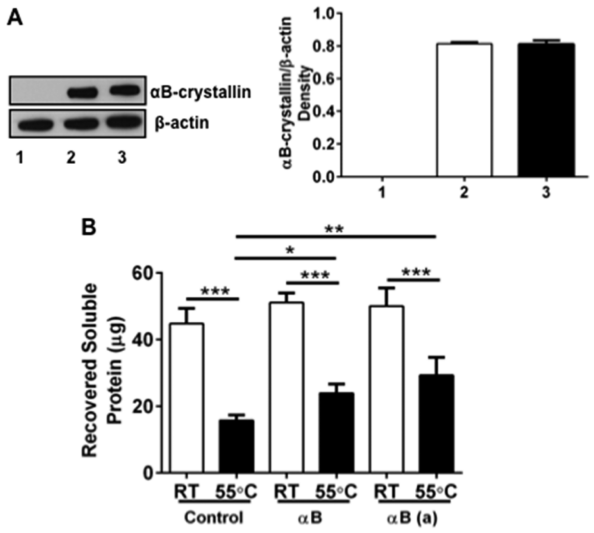

Figure 6. Chaperone activity of acetyl αB-crystallin is better than that of the native protein in HeLa cells. HeLa cells were transferred with native or acetyl αB-crystallin. (A) Western blotting and densitometry (bar graph) showed that the amount of protein transferred with the aid of BioPORTER was equal for the two proteins: lane 1, cell lysate; lane 2, cells transferred with native αB-crystallin; lane 3, cells transferred with acetyl αB-crystallin. (B) Cell lysates from αB-crystallin-transferred HeLa cells were incubated at 55 °C for 2 h, and the aggregated protein was removed by centrifugation. The protein content in the supernatant was measured. αB = native αB-crystallin. αB(a) = acetyl αB-crystallin. Bars are means ± SD of three independent experiments. *$p < 0.05$. **$p < 0.005$. ***$p < 0.0005$.

native protein ($p < 0.05$ compared to control) and further reduced to 41% with the transfer of the acetyl protein ($p < 0.005$ compared to control) (Figure 6B). Protein precipitation was not observed in any of the samples maintained at room temperature. Together, these data imply that the acetyl protein maintained stronger chaperone activity than the native protein.

We also determined the ability of the native and acetyl protein to refold denatured proteins, using MDH as the client protein. When fully denatured MDH was allowed to refold by being diluted in the appropriate refolding buffer (in the absence of αB-crystallin), a nominal 1% of the enzyme's activity was recovered (Figure 7, trace 1). However, in the presence of 20

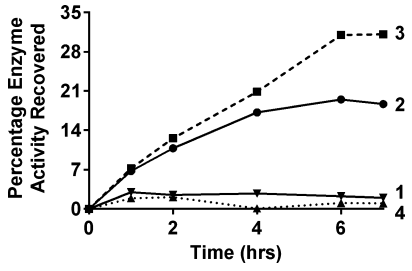

Figure 7. Effect of K92 acetylation on the ability of αB-crystallin to refold denatured MDH. The enzyme activity of MDH (which is directly related to protein refolding) was abolished by incubation in a 6 M Gu-HCl solution at 25 °C: trace 1, 10 nM MDH alone; trace 2, 10 nM MDH with 20 μM native αB-crystallin; trace 3, 10 nM MDH with 20 μM acetyl αB-crystallin; trace 4, 10 nM MDH with 20 μM BSA. Refolding was initiated by 100-fold dilution of MDH (1 μM) in 6 M Gu-HCl in refolding buffer (pH 7.5) containing 50 mM phosphate, 10 mM magnesium acetate, and 5 mM DTT. Each data point is the average of triplicate measurements.

μM native αB-crystallin, approximately 19% of the activity of MDH was regained (trace 2). At the same protein concentration, the recovery of the enzyme activity with acetyl αB-crystallin was 14% higher than with the native protein (trace 3). To rule out nonspecific effects, we used BSA in place of αB-crystallin, which had no effect on MDH refolding (trace 4). Thus, both the protein aggregation and the refolding assays showed that the acetylation of K92 improves the chaperone activity of αB-crystallin.

We measured the surface hydrophobicity using a hydrophobic probe, TNS, to determine whether an increase in the surface hydrophobicity resulted in a higher chaperone activity for the acetyl protein. The chaperone assays with Lyso, CS, MDH, and GC were conducted at 25, 43, 50, and 60 °C, respectively; therefore, we measured the surface hydrophobicity at these temperatures. As shown in Figure 8A, the fluorescence intensity of TNS bound to the acetyl protein was 11−20% higher than that of the native protein. These results suggest that K92 acetylation led to an increase in the hydrophobicity of the protein, which improved the chaperone activity of the protein.

To assess whether the improved chaperone activity is a result of stronger binding of the client protein to the acetyl protein, we performed an equilibrium binding study using GC as the client protein (Figure 8B). We determined the dissociation constant (K_d) using the Scatchard equation:

$$\tilde{\nu}/S = n/K_d - 1/K_d \times \tilde{\nu}$$

where $\tilde{\nu}$ is the number of moles of substrate bound per mole of chaperone, n is the number of binding sites, and K_d is the dissociation constant. We noted that the number of binding sites (n) per subunit of acetylated protein increased to 3.34 from 2.33 in the native protein and that the K_d decreased slightly from 2.81 μM in the native protein to 2.73 μM in the acetyl protein (Table 3). From these data, we conclude that the acetylation of K92 in αB-crystallin provides a higher affinity for denatured proteins. However, in these experiments, we cannot rule out aggregation and association of the client protein before it binds to αB-crystallin at 60 °C, which could result in a larger n per molecule of αB-crystallin.

Next, we investigated the effect of K92 acetylation on the second important function of αB-crystallin, its ability to prevent apoptosis in stressed cells. We used HeLa cells for these experiments because these cells contain low levels of endogenous αB-crystallin. The native and acetyl proteins were transferred into cells using BioPORTER. We induced apoptosis by treating the cells with either 100 nM staurosporine or 20 μM etoposide. As shown in panels A and B of Figure 9, both proteins significantly inhibited apoptosis. However, the acetyl protein was 18−20% more effective than the native protein in both treatments. The inhibition of apoptosis was accompanied by significant inhibition of caspase-3 activity in both treatments (Figure 9C,D). Again, the acetyl protein was at least 5−10% more effective than the native protein. Taken together, these results show that the acetylation of K92 makes αB-crystallin a more effective anti-apoptotic protein through stronger inhibition of caspase-3.

Molecular modeling based on the X-ray crystal structure of the ACD[47] shows that the removal of the positive charge on K92 by acetylation diminishes the electrostatic potential, changing this region from hydrophilic to hydrophobic. The resulting electrostatic potential in this area is neutral due to compensation by ionic interactions between neighboring residues glutamine 99 (Q99) and K90. The shape of the

dx.doi.org/10.1021/bi400638s | Biochemistry 2013, 52, 8126−8138

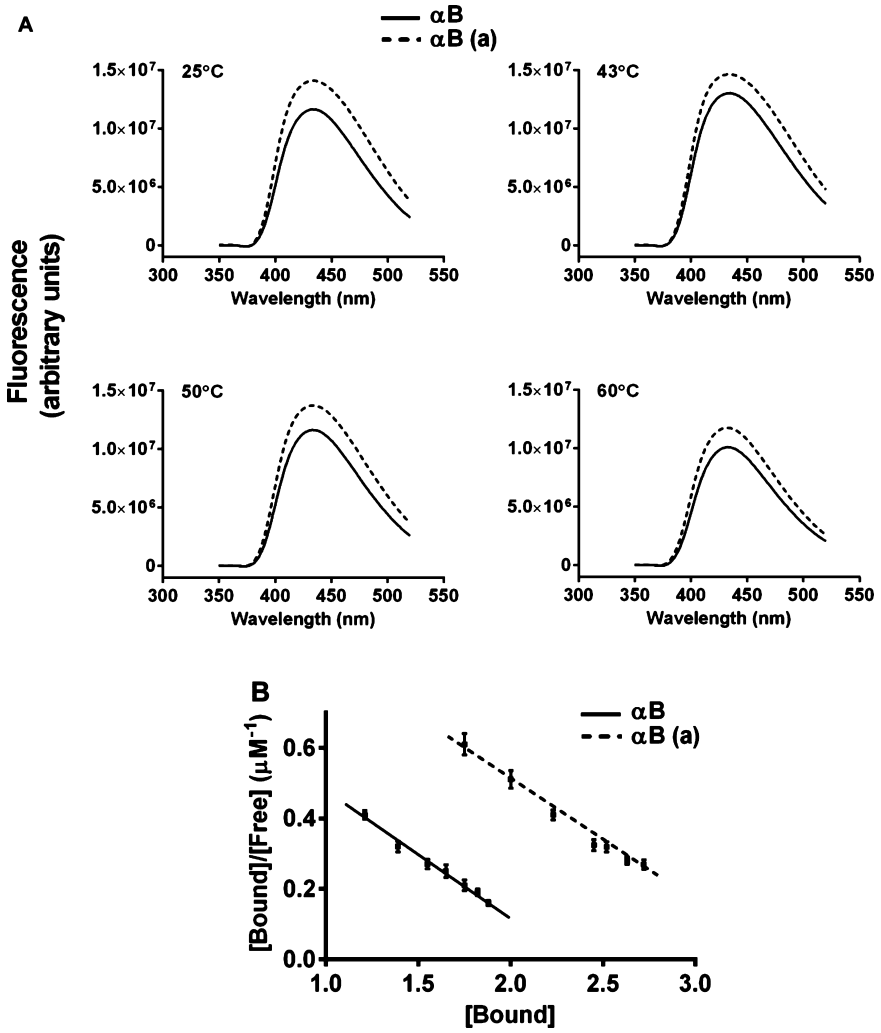

Figure 8. Surface hydrophobicity of acetyl αB-crystallin and estimation of binding parameters with client proteins. (A) Surface hydrophobicity probed with TNS at different temperatures. At all of the temperatures, the acetyl protein exhibited a higher surface hydrophobicity than the native protein. (B) The dissociation constant (K_d) and the number of binding sites (n) for the interaction between GC and αB-crystallin at 60 °C were estimated using the Scatchard equation shown in the Results. αB = native αB-crystallin. αB(a) = acetyl αB-crystallin.

Table 3. Determination of Values of n and K_d for the Interaction of Native and Acetyl αB-Crystallin with GC at 60 °C

	n	K_d (μM)
native with GC	2.33 ± 0.04	2.81 ± 0.14
acetyl with GC	3.34 ± 0.06	2.73 ± 0.19

electrostatic potential changed from a quadrupole to a dipole (Figure 10A,B), which can facilitate the formation of large oligomers of ACD. Changes are also visible on the molecular surface, mapped with electrostatic potential (Figure 10C,D). Thus, molecular modeling supports the finding that K92 acetylation makes αB-crystallin more hydrophobic and consequently a better chaperone.

DISCUSSION

Lysine acetylation is a dynamic process, regulated through KATs and KDACs. Several recent studies have shown that this process plays an important role in the regulation of metabolism and cell functions.[33,34] We previously found that αA- and αB-crystallin are acetylated at specific lysine residues in the lens.[37] The purpose of this study was to investigate the effects of lysine acetylation at K92 on the structure and functions of human αB-crystallin. This site was chosen on the basis of our previous finding that K92 is acetylated in the human lens[37] and because it is a highly conserved residue among several major small heat shock proteins.

Our previous *in vitro* lysine acetylation using a chemical method showed improvement in the chaperone and anti-apoptotic activity of α-crystallin.[37,38] However, in these studies, lysine acetylation was performed by reacting αA-crystallin with acetic anhydride. This method indiscriminately acetylates lysine residues in αA-crystallin even at low acetic anhydride concentrations. Thus, the method does not permit investigation of the effects of specific AcK residues in α-crystallin. To circumvent this problem in this study, we used the novel chemical method of Huang et al.[41] in which we used MTCA to introduce an AcK mimic at K92 by first mutating the lysine to cysteine and then converting the cysteine to MTCTK. Our mass spectrometric and Western blotting data confirmed that we have achieved this goal. The fact that MTCA had no effect on either the structure or function of WT αB-crystallin and that C92 was almost entirely converted into the AcK mimic allowed

dx.doi.org/10.1021/bi400638s | *Biochemistry* 2013, 52, 8126−8138

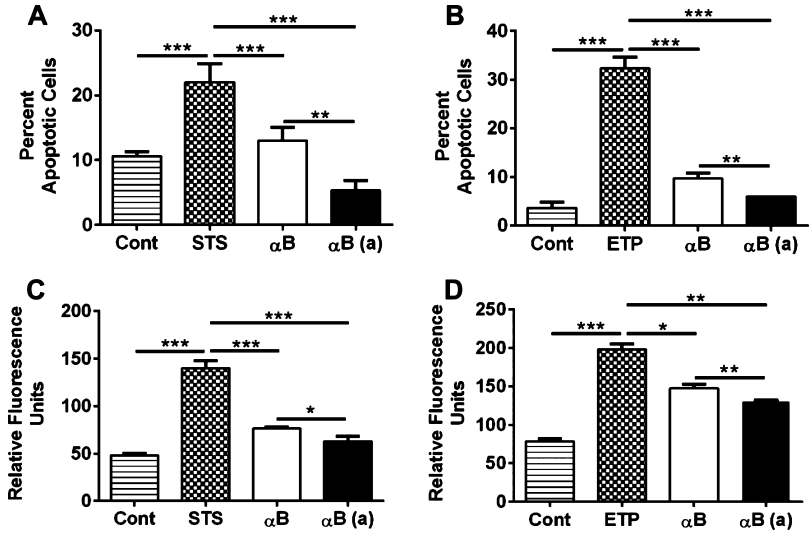

Figure 9. Inhibition of apoptosis by acetyl αB-crystallin was more effective than that by native αB-crystallin. Inhibition of staurosporine-induced (STS) (A) and etoposide-induced (ETP) (B) apoptosis in HeLa cells by the acetyl and native proteins. The protein was transferred with the aid of BioPORTER, and cells were treated with staurosporine and etoposide as described in Materials and Methods. Apoptosis was detected and quantified after staining for annexin V. The bars represent the means ± SD of three independent experiments. Acetyl αB-crystallin inhibits caspase-3 activity more aggressively than native αB-crystallin. Capase-3 activity in staurosporine (C) and etoposide (D) was measured using a fluorogenic substrate. αB = native αB-crystallin. αB(a) = acetyl αB-crystallin. The bars represent means ± SD of three independent experiments. *$p < 0.05$. **$p < 0.005$. ***$p < 0.0005$.

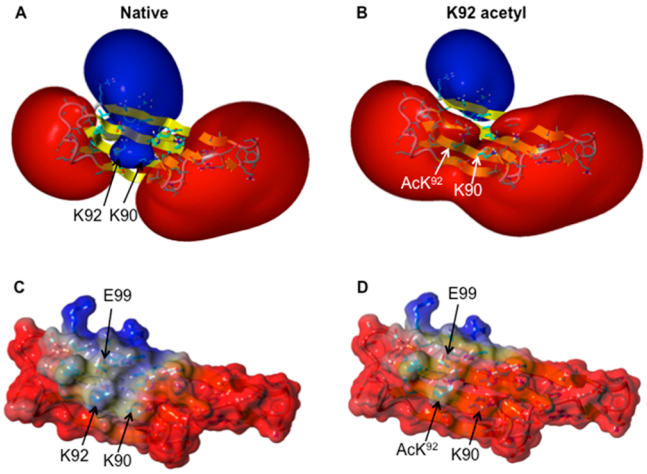

Figure 10. Molecular modeling of K92 acetylation in the ACD of αB-crystallin. Modeling was based on the published X-ray crystal structure of the ACD of αB-crystallin (PDB entry 2WJ7). The loss of the positive charge on the ε-amino group of K92, together with the electrostatic interaction of the neighboring lysine 90 and glutamic acid 99 residues, makes the average local charge zero in this area and changes the region from hydrophilic to hydrophobic. The electrostatic potentials for native (A) and acetyl αB-crystallin (B) are shown as isosurface blobs at levels of 25 kcal/mol (blue) and −25 kcal/mol (red). Molecular surface of crystallin mapped with the electrostatic potential for native (C) and acetyl αB-crystallin (D). The positive and negative electrostatic potentials on the isosurfaces and on the molecular surfaces are colored blue and red, respectively.

us to compare only native and acetyl αB-crystallin in subsequent experiments.

The alteration in the near-UV CD spectra and the greater tryptophan fluorescence intensity of the acetyl protein relative to that of the native protein (in light of the same emission maxima) suggest that K92 acetylation perturbs only the tertiary structure of αB-crystallin. This finding is analogous to our previous observation that lysine acetylation in αA-crystallin resulted in increased tryptophan fluorescence.[37] The two tryptophan residues (W9 and W60) in human αB-crystallin are located in the N-terminus of the protein, which is thought to be involved in monomeric interactions.[48] We speculate that the N-terminus is more relaxed in the acetyl protein, which results in the exposure of W9 and W60 to a more polar environment. Thus, the protein exhibits greater tryptophan fluorescence. Similarly, a previous study has shown changes in tryptophan fluorescence by subtle modifications in the ACD.[49]

The DLS−MALS data revealed that K92 acetylation led to an increase in the molecular mass and the hydrodynamic radius of the protein. The average molar mass of the acetyl protein almost doubled to 975 kDa (from 573 kDa for the native protein). This result implies that the acetyl protein exists in a larger oligomeric structure than the native protein. In α-crystallin, the core ACD is thought to be responsible for monomer interactions that lead to protein oligomerization.[50] The most favored model, based on solid state nuclear magnetic resonance spectroscopy and cryo-electron microscopy, is one in which the dimeric building blocks of αB-crystallin assemble into hexameric rings through ACD interactions and four such hexamers assemble through N-terminal interactions to form a 24-mer oligomer (one of many possible oligomeric structures) of αB-crystallin.[51] K92 is present within the ACD. Thus, its acetylation might enhance the oligomerization of the protein. However, monomeric interaction sites identified in previous studies do not contain K92.[48,52] Thus, the effect of K92 acetylation on the oligomerization could be a distal, secondary effect.

The increase in the chaperone activity of the acetyl protein is complemented by an increase in the surface hydrophobicity at four different temperatures. This finding indicates that the K92 acetylation that led to a larger oligomer of the protein might have contributed to the overall increase in surface hydrophobicity and, consequently, higher chaperone activity. The improved ability of the acetyl protein to refold a Gu-HCl-

dx.doi.org/10.1021/bi400638s | Biochemistry 2013, 52, 8126−8138

denatured protein (MDH) and the stronger binding of a client protein (GC) support this notion. K92 is located in strand β2 of the ACD in αB-crystallin. The results of the molecular modeling experiments are fully compatible with the surface hydrophobicity (TNS) and DLS−MALS data.

Previous studies did not establish a direct relationship between the chaperone activity and the oligomeric size of α-crystallin. In some studies, a lower molecular mass led to an improvement in chaperone activity,[53,54] but other studies have shown the opposite[55] or no relationship.[56] In this study, we found that subtle changes in surface hydrophobic patches and in the tertiary structure caused by K92 acetylation increased the oligomeric size of αB-crystallin. We also observed that such acetylation increased the overall structural stability by 7 kJ/mol. We believe that the larger oligomeric assembly and greater structural stability contributed to the improvement in the chaperone activity of acetyl αB-crystallin. This conclusion is similar to observations in other previous studies, where it has been noted that the increased chaperone activity of α-crystallin is associated with greater structural stability of the protein.[45,46]

The higher anti-apoptotic activity of the acetyl protein relative to that of the native protein could stem from its higher chaperone activity. We previously showed that the anti-apoptotic activity of α-crystallin is intricately linked to its chaperone function.[23] The higher anti-apoptotic activity of the acetyl protein could be due to its better ability to block the translocation of Bax to mitochondria, to release of cytochrome *c* into the cytoplasm, and to prevent caspase-8- and caspase-9-mediated activation of caspase-3. Further work is needed to verify these possibilities. The acetyl protein may more effectively preserve the cytoskeletal network, as αB-crystallin is known to bind cytoskeletal proteins and prevent their destabilization when cells are experiencing stress.[57] Whether lysine acetylation in αB-crystallin is reversed by lysine deacetylase in eye tissues is not known. Investigation into the enzymatic regulation of lysine acetylation should provide further insight into the role of this chemical modification in the functions of αB-crystallin.

What is the significance of our findings to lens and retinal biology? In the lens, negligible turnover of protein occurs; therefore, proteins have to be preserved in their native state to maintain transparency despite being exposed to sustained and chronic stresses. Acetylation of αB-crystallin could be a mechanism for enhancing the chaperone activity and reducing the level of aggregation of proteins. In addition, apoptosis of lens epithelial cells is a common occurrence during cataract formation,[58,59] which may be inhibited to a greater extent by the acetyl protein than by native αB-crystallin. Similarly, acetylation of αB-crystallin in the retina could help in preventing apoptosis of cells, which occurs in diseases such as macular degeneration, glaucoma, and diabetic retinopathy.

■ ASSOCIATED CONTENT

Supporting Information

Detection of acetyl αB-crystallin in human and mouse retinas, amino acid sequence alignment to show the conservation of K92 in small heat shock proteins, the effect of MTCA on αB-crystallin's structure and function, chaperone activity of acetyl αB-crystallin at different client protein:chaperone ratios, and the effect of time and αB-crystallin concentration on the thermal aggregation of HeLa cell proteins. This material is available free of charge via the Internet at http://pubs.acs.org.

■ AUTHOR INFORMATION

Corresponding Authors

*Department of Ophthalmology and Visual Sciences, Case Western Reserve University School of Medicine, Pathology Building, Room 301, 2085 Adelbert Rd., Cleveland, OH 44106. E-mail: ram.nagaraj@case.edu.

*School of Basic Sciences, Indian Institute of Technology Bhubaneswar, Bhubaneswar 751013, India. E-mail: abiswas@iitbbs.ac.in.

Funding

This study was supported by National Institutes of Health Grants R01EY-022061, R01EY-023286 (R.H.N.), and P30EY-11373 [Visual Sciences Research Center of Case Western Reserve University (CWRU)]; Research to Prevent Blindness, NY (to CWRU and the University of Missouri); The Ohio Lions Eye Research Foundation; and CSIR India Grant 37(1535)/12/EMR-II (A.B.). S.K.N. acknowledges the receipt of an Institute Fellowship from Indian Institute of Technology Bhubaneswar. This work was also supported by Grant N N401 557840 from Polish Ministry of Science and Higher Education (S.F.).

Notes

The authors declare no competing financial interest.

■ ACKNOWLEDGMENTS

We thank Dr. Irina Pikuleva for the human retinal specimen and Dr. Scott Howell for help with immunohistochemistry.

■ ABBREVIATIONS

AcK, N^{ε}-acetyllysine; MTCA, methylthiocarbonyl aziridine; MTCTK, methylthiocarbonyl thialysine; CS, citrate synthase; MDH, malate dehydrogenase; GC, γ-crystallin; Lyso, lysozyme; TNS, 2-(*p*-toluidinyl)naphthalene-6-sulfonic acid sodium salt; Gu-HCl, guanidine hydrochloride; DLS−MALS, dynamic light scattering−multiangle light scattering; STS, staurosporine; ETP, etoposide; KAT, lysine acetyltransferase; PTEN, phosphatase and tensin homologue; RPE, retinal pigmented epithelial.

■ REFERENCES

(1) Clark, A. R., Lubsen, N. H., and Slingsby, C. (2012) sHSP in the eye lens: Crystallin mutations, cataract and proteostasis. *Int. J. Biochem. Cell Biol. 44*, 1687−1697.

(2) Horwitz, J. (2003) α-Crystallin. *Exp. Eye Res. 76*, 145−153.

(3) Basha, E., O'Neill, H., and Vierling, E. (2012) Small heat shock proteins and α-crystallins: Dynamic proteins with flexible functions. *Trends Biochem. Sci. 37*, 106−117.

(4) Peterson, J., Radke, G., and Takemoto, L. (2005) Interaction of lens α and γ crystallins during aging of the bovine lens. *Exp. Eye Res. 81*, 680−689.

(5) Acunzo, J., Katsogiannou, M., and Rocchi, P. (2012) Small heat shock proteins HSP27 (HspB1), αB-crystallin (HspB5) and HSP22 (HspB8) as regulators of cell death. *Int. J. Biochem. Cell Biol. 44*, 1622−1631.

(6) Song, S., Hanson, M. J., Liu, B. F., Chylack, L. T., and Liang, J. J. (2008) Protein-protein interactions between lens vimentin and αB-crystallin using FRET acceptor photobleaching. *Mol. Vis. 14*, 1282−1287.

(7) Nicholl, I. D., and Quinlan, R. A. (1994) Chaperone activity of α-crystallins modulates intermediate filament assembly. *EMBO J. 13*, 945−953.

(8) Truscott, R. J., Comte-Walters, S., Ablonczy, Z., Schwacke, J. H., Berry, Y., Korlimbinis, A., Friedrich, M. G., and Schey, K. L. (2011)

Tight binding of proteins to membranes from older human cells. *Age 33*, 543−554.
(9) Xi, J. H., Bai, F., McGaha, R., and Andley, U. P. (2006) α-Crystallin expression affects microtubule assembly and prevents their aggregation. *FASEB J. 20*, 846−857.
(10) Inaguma, Y., Ito, H., Iwamoto, I., Saga, S., and Kato, K. (2001) αB-Crystallin phosphorylated at Ser-59 is localized in centrosomes and midbodies during mitosis. *Eur. J. Cell Biol. 80*, 741−748.
(11) Gangalum, R. K., Schibler, M. J., and Bhat, S. P. (2004) Small heat shock protein αB-crystallin is part of cell cycle-dependent Golgi reorganization. *J. Biol. Chem. 279*, 43374−43377.
(12) Boyle, D. L., Takemoto, L., Brady, J. P., and Wawrousek, E. F. (2003) Morphological characterization of the αA- and αB-crystallin double knockout mouse lens. *BMC Ophthalmol. 3*, 3.
(13) Brady, J. P., Garland, D., Duglas-Tabor, Y., Robison, W. G., Jr., Groome, A., and Wawrousek, E. F. (1997) Targeted disruption of the mouse αA-crystallin gene induces cataract and cytoplasmic inclusion bodies containing the small heat shock protein αB-crystallin. *Proc. Natl. Acad. Sci. U.S.A. 94*, 884−889.
(14) Andley, U. P., Hamilton, P. D., Ravi, N., and Weihl, C. C. (2011) A knock-in mouse model for the R120G mutation of αB-crystallin recapitulates human hereditary myopathy and cataracts. *PLoS One 6*, e17671.
(15) Hsu, C. D., Kymes, S., and Petrash, J. M. (2006) A transgenic mouse model for human autosomal dominant cataract. *Invest. Ophthalmol. Visual Sci. 47*, 2036−2044.
(16) Rekas, A., Adda, C. G., Andrew Aquilina, J., Barnham, K. J., Sunde, M., Galatis, D., Williamson, N. A., Masters, C. L., Anders, R. F., Robinson, C. V., Cappai, R., and Carver, J. A. (2004) Interaction of the molecular chaperone αB-crystallin with α-synuclein: Effects on amyloid fibril formation and chaperone activity. *J. Mol. Biol. 340*, 1167−1183.
(17) Ecroyd, H., and Carver, J. A. (2009) Crystallin proteins and amyloid fibrils. *Cell. Mol. Life Sci. 66*, 62−81.
(18) Wang, X., Osinska, H., Klevitsky, R., Gerdes, A. M., Nieman, M., Lorenz, J., Hewett, T., and Robbins, J. (2001) Expression of R120G-αB-crystallin causes aberrant desmin and αB-crystallin aggregation and cardiomyopathy in mice. *Circ. Res. 89*, 84−91.
(19) Rothbard, J. B., Kurnellas, M. P., Brownell, S., Adams, C. M., Su, L., Axtell, R. C., Chen, R., Fathman, C. G., Robinson, W. H., and Steinman, L. (2012) Therapeutic effects of systemic administration of chaperone αB-crystallin associated with binding proinflammatory plasma proteins. *J. Biol. Chem. 287*, 9708−9721.
(20) Ousman, S. S., Tomooka, B. H., van Noort, J. M., Wawrousek, E. F., O'Connor, K. C., Hafler, D. A., Sobel, R. A., Robinson, W. H., and Steinman, L. (2007) Protective and therapeutic role for αB-crystallin in autoimmune demyelination. *Nature 448*, 474−479.
(21) Kurnellas, M. P., Brownell, S. E., Su, L., Malkovskiy, A. V., Rajadas, J., Dolganov, G., Chopra, S., Schoolnik, G. K., Sobel, R. A., Webster, J., Ousman, S. S., Becker, R. A., Steinman, L., and Rothbard, J. B. (2012) Chaperone activity of small heat shock proteins underlies therapeutic efficacy in experimental autoimmune encephalomyelitis. *J. Biol. Chem. 287*, 36423−36434.
(22) Fort, P. E., and Lampi, K. J. (2011) New focus on α-crystallins in retinal neurodegenerative diseases. *Exp. Eye Res. 92*, 98−103.
(23) Pasupuleti, N., Matsuyama, S., Voss, O., Doseff, A. I., Song, K., Danielpour, D., and Nagaraj, R. H. (2010) The anti-apoptotic function of human αA-crystallin is directly related to its chaperone activity. *Cell Death Dis. 1*, e31.
(24) Kamradt, M. C., Chen, F., and Cryns, V. L. (2001) The small heat shock protein αB-crystallin negatively regulates cytochrome c- and caspase-8-dependent activation of caspase-3 by inhibiting its autoproteolytic maturation. *J. Biol. Chem. 276*, 16059−16063.
(25) Sreekumar, P. G., Kannan, R., Kitamura, M., Spee, C., Barron, E., Ryan, S. J., and Hinton, D. R. (2010) αB-Crystallin is apically secreted within exosomes by polarized human retinal pigment epithelium and provides neuroprotection to adjacent cells. *PLoS One 5*, e12578.
(26) Bhat, S. P., and Gangalum, R. K. (2011) Secretion of αB-crystallin via exosomes: New clues to the function of human retinal pigment epithelium. *Commun. Integr. Biol. 4*, 739−741.
(27) Kannan, R., Sreekumar, P. G., and Hinton, D. R. (2012) Novel roles for α-crystallins in retinal function and disease. *Prog. Retinal Eye Res. 31*, 576−604.
(28) Losiewicz, M. K., and Fort, P. E. (2011) Diabetes impairs the neuroprotective properties of retinal α-crystallins. *Invest. Ophthalmol. Visual Sci. 52*, 5034−5042.
(29) Adhikari, A. S., Sridhar Rao, K., Nagaraj, R., Parnaik, V. K., and Mohan Rao, C. (2004) Heat stress-induced localization of small heat shock proteins in mouse myoblasts: Intranuclear lamin A/C speckles as target for αB-crystallin and Hsp25. *Exp. Cell Res. 299*, 393−403.
(30) McGreal, R. S., Kantorow, W. L., Chauss, D. C., Wei, J., Brennan, L. A., and Kantorow, M. (2012) αB-Crystallin/sHSP protects cytochrome c and mitochondrial function against oxidative stress in lens and retinal cells. *Biochim. Biophys. Acta 1820*, 921−930.
(31) Sadoul, K., Wang, J., Diagouraga, B., and Khochbin, S. (2011) The tale of protein lysine acetylation in the cytoplasm. *J. Biomed. Biotechnol. 2011*, 970382.
(32) Yang, X. J., and Seto, E. (2008) Lysine acetylation: Codified crosstalk with other posttranslational modifications. *Mol. Cell 31*, 449−461.
(33) Zhao, S., Xu, W., Jiang, W., Yu, W., Lin, Y., Zhang, T., Yao, J., Zhou, L., Zeng, Y., Li, H., Li, Y., Shi, J., An, W., Hancock, S. M., He, F., Qin, L., Chin, J., Yang, P., Chen, X., Lei, Q., Xiong, Y., and Guan, K. L. (2010) Regulation of cellular metabolism by protein lysine acetylation. *Science 327*, 1000−1004.
(34) Choudhary, C., Kumar, C., Gnad, F., Nielsen, M. L., Rehman, M., Walther, T. C., Olsen, J. V., and Mann, M. (2009) Lysine acetylation targets protein complexes and co-regulates major cellular functions. *Science 325*, 834−840.
(35) Lin, P. P., Barry, R. C., Smith, D. L., and Smith, J. B. (1998) In vivo acetylation identified at lysine 70 of human lens αA-crystallin. *Protein Sci. 7*, 1451−1457.
(36) Lapko, V. N., Smith, D. L., and Smith, J. B. (2001) In vivo carbamylation and acetylation of water-soluble human lens αB-crystallin lysine 92. *Protein Sci. 10*, 1130−1136.
(37) Nagaraj, R. H., Nahomi, R. B., Shanthakumar, S., Linetsky, M., Padmanabha, S., Pasupuleti, N., Wang, B., Santhoshkumar, P., Panda, A. K., and Biswas, A. (2012) Acetylation of αA-crystallin in the human lens: Effects on structure and chaperone function. *Biochim. Biophys. Acta 1822*, 120−129.
(38) Nahomi, R. B., Oya-Ito, T., and Nagaraj, R. H. (2013) The combined effect of acetylation and glycation on the chaperone and anti-apoptotic functions of human α-crystallin. *Biochim. Biophys. Acta 1832*, 195−203.
(39) Wang, X., and Hayes, J. J. (2008) Acetylation mimics within individual core histone tail domains indicate distinct roles in regulating the stability of higher-order chromatin structure. *Mol. Cell. Biol. 28*, 227−236.
(40) Scroggins, B. T., Robzyk, K., Wang, D., Marcu, M. G., Tsutsumi, S., Beebe, K., Cotter, R. J., Felts, S., Toft, D., Karnitz, L., Rosen, N., and Neckers, L. (2007) An acetylation site in the middle domain of Hsp90 regulates chaperone function. *Mol. Cell 25*, 151−159.
(41) Huang, R., Holbert, M. A., Tarrant, M. K., Curtet, S., Colquhoun, D. R., Dancy, B. M., Dancy, B. C., Hwang, Y., Tang, Y., Meeth, K., Marmorstein, R., Cole, R. N., Khochbin, S., and Cole, P. A. (2010) Site-specific introduction of an acetyl-lysine mimic into peptides and proteins by cysteine alkylation. *J. Am. Chem. Soc. 132*, 9986−9987.
(42) Biswas, A., and Das, K. P. (2007) Differential recognition of natural and nonnatural substrate by molecular chaperone α-crystallin-A subunit exchange study. *Biopolymers 85*, 189−197.
(43) Nagaraj, R. H., Panda, A. K., Shanthakumar, S., Santhoshkumar, P., Pasupuleti, N., Wang, B., and Biswas, A. (2012) Hydroimidazolone modification of the conserved Arg12 in small heat shock proteins: Studies on the structure and chaperone function using mutant mimics. *PLoS One 7*, e30257.

(44) Pasupuleti, N., Gangadhariah, M., Padmanabha, S., Santhoshkumar, P., and Nagaraj, R. H. (2010) The role of the cysteine residue in the chaperone and anti-apoptotic functions of human Hsp27. *J. Cell. Biochem. 110*, 408−419.
(45) Biswas, A., Goshe, J., Miller, A., Santhoshkumar, P., Luckey, C., Bhat, M. B., and Nagaraj, R. H. (2007) Paradoxical effects of substitution and deletion mutation of Arg56 on the structure and chaperone function of human αB-crystallin. *Biochemistry 46*, 1117−1127.
(46) Biswas, A., and Das, K. P. (2004) Role of ATP on the interaction of α-crystallin with its substrates and its implications for the molecular chaperone function. *J. Biol. Chem. 279*, 42648−42657.
(47) Bagneris, C., Bateman, O. A., Naylor, C. E., Cronin, N., Boelens, W. C., Keep, N. H., and Slingsby, C. (2009) Crystal structures of α-crystallin domain dimers of αB-crystallin and Hsp20. *J. Mol. Biol. 392*, 1242−1252.
(48) Ghosh, J. G., and Clark, J. I. (2005) Insights into the domains required for dimerization and assembly of human αB-crystallin. *Protein Sci. 14*, 684−695.
(49) Liu, Y., Zhang, X., Luo, L., Wu, M., Zeng, R., Cheng, G., Hu, B., Liu, B., Liang, J. J., and Shang, F. (2006) A novel αB-crystallin mutation associated with autosomal dominant congenital lamellar cataract. *Invest. Ophthalmol. Visual Sci. 47*, 1069−1075.
(50) Berengian, A. R., Parfenova, M., and McHaourab, H. S. (1999) Site-directed spin labeling study of subunit interactions in the α-crystallin domain of small heat-shock proteins. Comparison of the oligomer symmetry in αA-crystallin, HSP 27, and HSP 16.3. *J. Biol. Chem. 274*, 6305−6314.
(51) Delbecq, S. P., and Klevit, R. E. (2013) One size does not fit all: The oligomeric states of αB-crystallin. *FEBS Lett. 587*, 1073−1080.
(52) Sreelakshmi, Y., and Sharma, K. K. (2005) Recognition sequence 2 (residues 60−71) plays a role in oligomerization and exchange dynamics of αB-crystallin. *Biochemistry 44*, 12245−12252.
(53) Santhoshkumar, P., Murugesan, R., and Sharma, K. K. (2009) Deletion of (54)FLRAPSWF(61) residues decreases the oligomeric size and enhances the chaperone function of αB-crystallin. *Biochemistry 48*, 5066−5073.
(54) Pasta, S. Y., Raman, B., Ramakrishna, T., and Rao, Ch. M. (2003) Role of the conserved SRLFDQFFG region of α-crystallin, a small heat shock protein. Effect on oligomeric size, subunit exchange, and chaperone-like activity. *J. Biol. Chem. 278*, 51159−51166.
(55) Kumar, L. V., and Rao, C. M. (2000) Domain swapping in human αA- and αB-crystallins affects oligomerization and enhances chaperone-like activity. *J. Biol. Chem. 275*, 22009−22013.
(56) Saha, S., and Das, K. P. (2007) Unfolding and refolding of bovine α-crystallin in urea and its chaperone activity. *Protein J. 26*, 315−326.
(57) Wettstein, G., Bellaye, P. S., Micheau, O., and Bonniaud, P. (2012) Small heat shock proteins and the cytoskeleton: An essential interplay for cell integrity? *Int. J. Biochem. Cell Biol. 44*, 1680−1686.
(58) Li, W. C., Kuszak, J. R., Dunn, K., Wang, R. R., Ma, W., Wang, G. M., Spector, A., Leib, M., Cotliar, A. M., Weiss, M., et al. (1995) Lens epithelial cell apoptosis appears to be a common cellular basis for non-congenital cataract development in humans and animals. *J. Cell Biol. 130*, 169−181.
(59) Takamura, Y., Kubo, E., Tsuzuki, S., and Akagi, Y. (2003) Apoptotic cell death in the lens epithelium of rat sugar cataract. *Exp. Eye Res. 77*, 51−57.